

See discussions, stats, and author profiles for this publication at: <https://www.researchgate.net/publication/272269992>

Selective Ion Transport through Functionalized Graphene Membranes Based on Delicate Ion–Graphene Interactions

ARTICLE *in* THE JOURNAL OF PHYSICAL CHEMISTRY C · AUGUST 2014

Impact Factor: 4.77 · DOI: 10.1021/jp504921p

CITATIONS

2

READS

22

6 AUTHORS, INCLUDING:



Pengzhan Sun

Tsinghua University

28 PUBLICATIONS 389 CITATIONS

SEE PROFILE



Kunlin Wang

Tsinghua University

203 PUBLICATIONS 4,720 CITATIONS

SEE PROFILE



Minlin Zhong

Tsinghua University

158 PUBLICATIONS 1,259 CITATIONS

SEE PROFILE

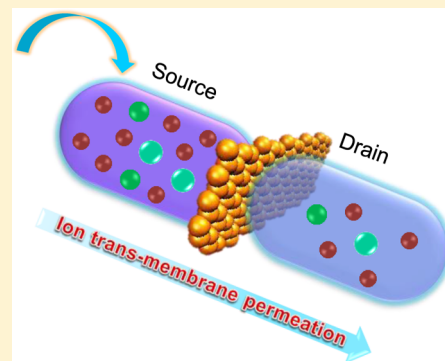
Selective Ion Transport through Functionalized Graphene Membranes Based on Delicate Ion–Graphene Interactions

Pengzhan Sun,[†] He Liu,[‡] Kunlin Wang,[†] Minlin Zhong,[†] Dehai Wu,[‡] and Hongwei Zhu^{*,†,§}

[†]School of Materials Science and Engineering, State Key Laboratory of New Ceramics and Fine Processing, Key Laboratory of Materials Processing Technology of MOE, [‡]Department of Mechanical Engineering, and [§]Center for Nano and Micro Mechanics, Tsinghua University, Beijing 100084, China

S Supporting Information

ABSTRACT: Recently, graphene oxide (GO) membranes have been reported with the ability to separate different solutes in aqueous suspensions by a molecular sieving effect. On the other hand, we propose that the chemical interactions between ions and GO membranes might also take effect in selective ion transmembrane transportation. In this paper, on the basis of the permeation of Cu^{2+} and Mg^{2+} sources through hydroxyl-, carboxyl-, and amino-functionalized graphene membranes, the delicate ion–graphene interactions which might be responsible for the selective ion permeation are investigated. We demonstrate experimentally that the coordination between transition-metal cations and carboxyl functionalities and the cation– π interactions between main-group cations and sp^2 regions are responsible for the selective transport of small ions through graphene-based membranes, which is beyond the scope of molecular sieving effect proposed previously. Notably, by grafting amino groups onto the graphene basal planes, the permeations of Cu^{2+} and Mg^{2+} cations are both weakened. These results not only throw light upon the mechanism for the selective ion permeation through graphene-based membranes but also lay a foundation for the separation of target ions by grafting specific functionalities.



Nanoporous graphene^{1–3} or graphene oxide (GO) membranes^{4–7} have been demonstrated to be excellent barrier materials in recent years, which hold great promises in filtration and separation. Specially, because of the characteristics of easy to synthesize and to produce in large scale,^{8,9} GO membranes are particularly attractive for practical industrial applications. In terms of the structure of GO sheet, it can be viewed as a 2-dimensional carbon lattice consisting of clustered nano- sp^2 regions and sp^3 hybridized C–O matrix.^{10,11} When a large amount of single-layered GO sheets are stacked together to form the micrometer-thick GO membranes, a network of sp^2 nanocapillaries can be formed by connecting all the sp^2 clusters together across the whole stacked laminates through which water vapors can afford an unimpeded permeation⁶ on the basis of the formation of ice bilayer and the melting transition at the edges of GO flakes,¹² while other liquids or gases can be blocked completely. In contrast, if only a few layers of GO flakes are stacked to form the nanometer-thick membranes, the continuous graphitic nanocapillaries are difficult to form and mass transport happens mostly through the structural defects within the flakes.^{4,5} Interestingly, an ultrahigh selectivity toward different gases can be achieved by the as-fabricated nanometer-thick GO membranes, making them suitable for CO_2 capture and practical H_2 separation.^{4,5} More recently, Joshi et al. have reported that micrometer-thick GO membranes can be used to separate different solutes in solutions by a molecular sieving effect with an ultrafast speed through which molecules or ions with a hydrated radii > 4.5 Å can be blocked completely.⁷ On

the other hand, for the small metal cations in solutions (hydrated radii < 4.5 Å), we have proposed previously that the delicate chemical interactions between ions and GO sheets might be responsible for the ion-selectivity of GO membranes.^{13–15} However, these conclusions are mostly extrapolated from the permeation behaviors of diverse ions through the identical GO membranes, and direct experimental evidence for them are lacking thus far.

In this work, the diverse chemical interactions between metal cations and GO membranes, which might be responsible for the ion-selectivity of GO membranes beyond the functioning stage of molecular sieving effect (hydrated radii < 4.5 Å), are investigated by comparing the permeation properties of Cu^{2+} (transition-metal cation) and Mg^{2+} (main-group cation) sources through hydroxyl-, carboxyl-, and amino-functionalized graphene membranes.

GO flakes were synthesized by the typical modified Hummers' method with natural graphitic flakes.¹⁶ Hydroxyl-, carboxyl-, and amino-functionalized graphene (named as "G–OH", "G–COOH", and "G–NH₂") sheets were prepared on the basis of the as-synthesized GO flakes according to the previous methods.^{17–19} Figure S1 shows the photographs and scanning electron microscopy (SEM) images of the as-

Received: May 19, 2014

Revised: July 29, 2014

Published: July 29, 2014

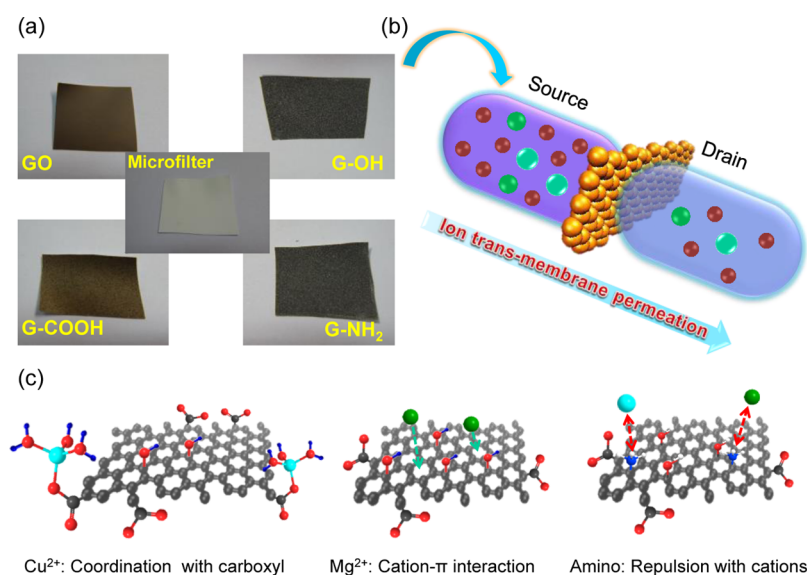


Figure 1. (a) Photographs of the blank microfilter, as-fabricated GO, G-OH, G-COOH, and G-NH₂ membranes. (b) Schematic diagram of the ion transmembrane permeation process through functionalized graphene membranes. (c) The proposed mechanism for the diverse chemical interactions between ions and functionalized graphene.

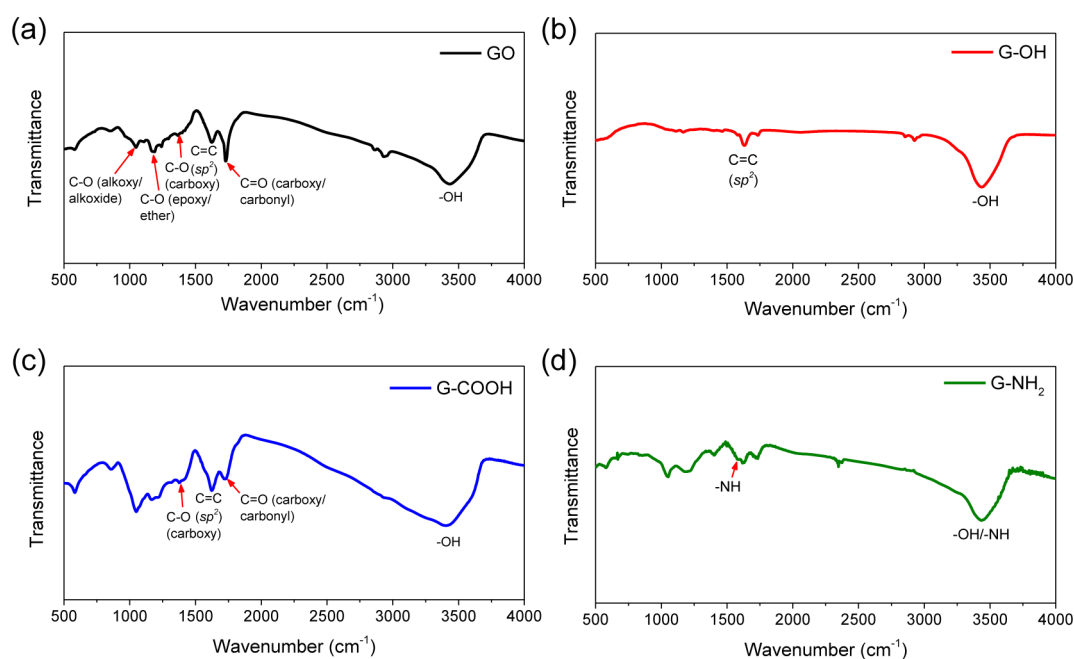


Figure 2. FTIR spectra of (a) GO, (b) G-OH, (c) G-COOH, and (d) G-NH₂ membranes.

synthesized GO, G-OH, G-COOH, and G-NH₂ powders. It reveals that after further chemical conversion of GO, the as-synthesized functionalized graphene (G-OH, G-COOH, and G-NH₂) powders possess rather different topographies from GO. After the preparation procedures, GO, G-OH, and G-COOH flakes were dispersed in deionized water, while G-NH₂ flakes were dispersed in ethanol by sonication to form the 0.1 mg/mL preparation solutions. The SEM characterizations of the well-exfoliated GO, G-OH, G-COOH, and G-NH₂ flakes are present in Figure S2 of the Supporting Information, showing the micrometer-sized lateral dimensions of the as-prepared functionalized graphene flakes. With these graphene-based flakes in hand, the continuous GO, G-OH, G-COOH, and G-NH₂ membrane filters were fabricated by vacuum-

filtration with the commonly used cellulose microfilters (pore size: ~220 nm, porosity: ~80%) from 25 mL, 0.1 mg/mL preparation solutions. Figure 1a shows the photographs of the as-fabricated GO, G-OH, G-COOH, and G-NH₂ membranes with the polymeric microfilters underneath. The cellulose microfilter is also included in Figure 1a for comparison. On the basis of these functionalized graphene membranes, a series of ion permeation experiments were conducted with a homemade apparatus (see Supporting Information), similar to our previous work,^{13–15} as illustrated in Figure 1b. To exclude the effect of the polymeric substrates underneath, control experiments were done with blank microfilters. In the ion permeation experiments, 80 mL of 0.1 mol/L certain electrolytes and deionized water were injected

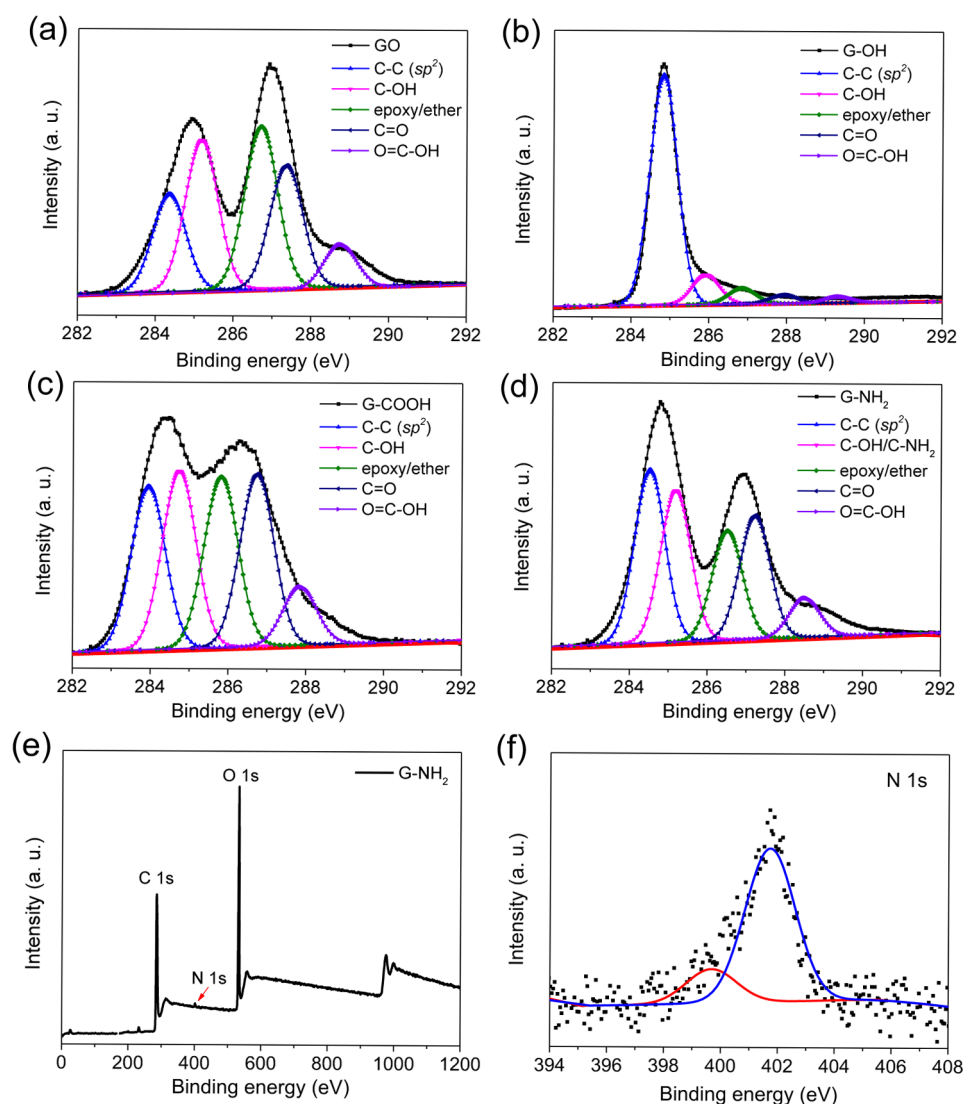


Figure 3. C 1s XPS spectra of (a) GO, (b) G–OH, (c) G–COOH, and (d) G–NH₂ membranes. (e) XPS spectrum of G–NH₂ membranes over a wide range of binding energies (0–1200 eV). (f) N 1s spectrum of G–NH₂ membranes. The black dots are experimental plots; the red and blue lines are fitting curves.

into the source and drain reservoirs, respectively, with the same speed to ensure that no external hydrostatic pressures were applied across the membrane. The whole ion transmembrane permeation process was conducted under mild magnetic stirring to eliminate the possible concentration gradients near the membranes. The cation concentrations in the drain solutions were measured by atomic emission spectroscopy at regular intervals (30 min) to quantify the ion permeation behavior through graphene-based membranes. The ion permeation experiments were specially performed with Cu²⁺ and Mg²⁺ chlorides to study the possible chemical interactions of transition-metal cations and main-group cations with the functionalized graphene membranes (illustrated in Figure 1c) on the basis of the following reasons: (1) they represent typical transition metallic cations and main-group metallic cations and (2) they possess the same positive charges and similar naked ion radii and hydrated ion radii.

First, Fourier transform infrared (FTIR) spectroscopy and X-ray photoelectron spectrometer (XPS) were utilized to study the chemical compositions of the as-prepared GO, G–OH, G–COOH, and G–NH₂ membranes, as shown in Figures 2 and 3.

They reveal that GO membranes are attached with plenty of oxygen-containing functional groups (e.g., C–O, C–OH, and C=O) (Figures 2a and 3a), while for the case of G–OH membranes, only a small portion of hydroxyl and epoxy/ether groups are decorated (Figures 2b and 3b). Notably, the atomic percentage of sp² C–C bonds in the G–OH case is significantly enhanced compared to GO membranes, just similar to the chemically or thermally reduced cases. Therefore, with the G–OH membranes, the possible cation– π interactions between metallic cations and sp² graphitic clusters¹⁴ can be investigated on the basis of ion transmembrane permeations. On the other hand, according to the FTIR and XPS spectra of G–COOH membranes shown in Figures 2c and 3c, the atomic ratio of carboxyl functional groups is enhanced significantly compared to GO membranes, indicating that with G–COOH membranes the possible coordination interactions between transition-metal cations and carboxyl functionalities,¹³ which might be responsible for the recognition of transition-metal cations by graphene-based membranes, can be demonstrated. In addition, according to the FTIR and XPS spectra of G–NH₂ membranes (Figures 2d and 3d–f), it can be concluded that a trace amount

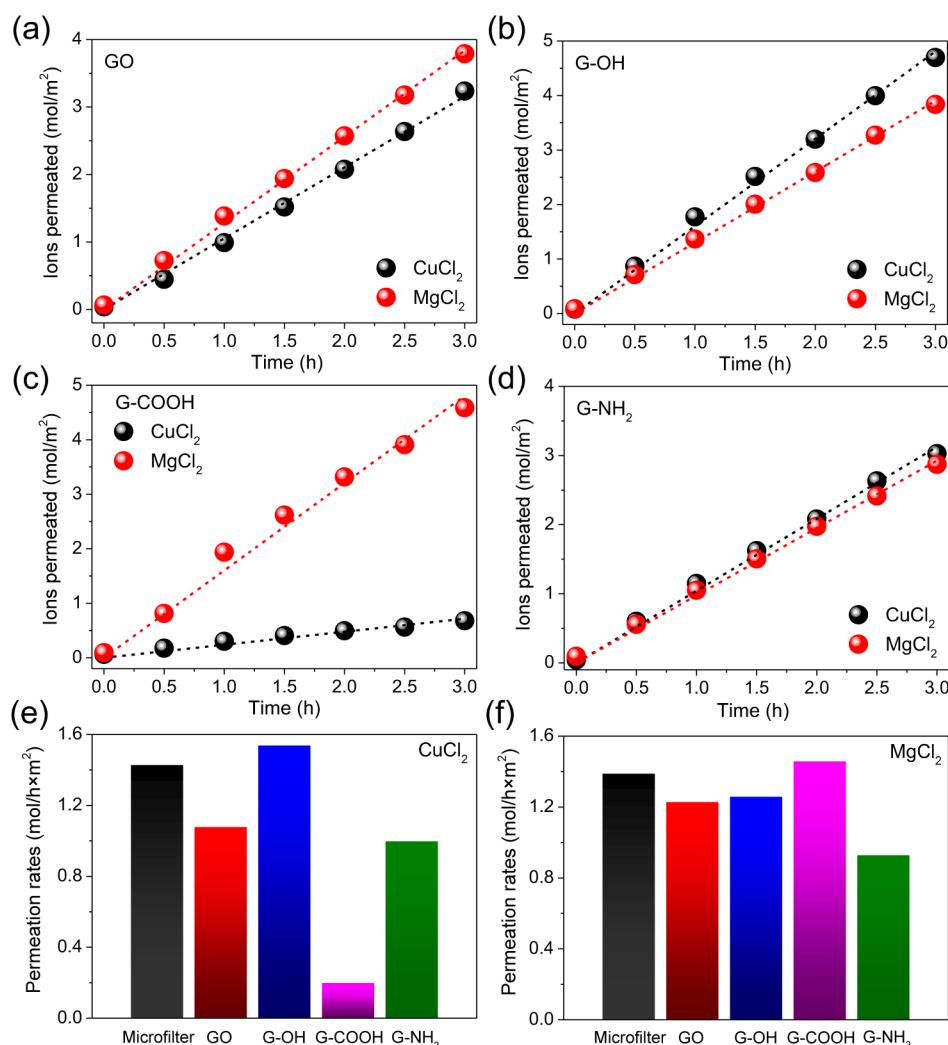


Figure 4. Permeations of CuCl_2 and MgCl_2 sources through (a) GO, (b) G-OH, (c) G-COOH, and (d) G-NH₂ membranes. The plots are averaged on the basis of at least three data, and the variations of the data are within the sizes of the data balls. The dotted lines are linear fits. (e) Cu^{2+} and (f) Mg^{2+} permeation rates through blank microfilters, GO, G-OH, G-COOH, and G-NH₂ membranes with the cellulose microfilters underneath.

of amino functional groups is grafted onto the graphene flakes and that the atomic percentage of N, which is defined as 100 N/C at.%, can be calculated as $\sim 1.97\%$. Because of the effective attraction of H^+ by the N atoms in amino functionalities in aqueous environment, they will be charged positively, which facilitates the investigation of electrostatic interactions between ions and functionalized graphene membranes.

Next, on the basis of these functionalized graphene membranes, the transmembrane permeation properties of CuCl_2 and MgCl_2 are studied. As shown in Figure 4, the permeations of Cu^{2+} and Mg^{2+} ions through GO, G-OH, G-COOH, and G-NH₂ membranes are compared separately to explore the possible interactions of transition-metal cations and main-group cations with different functionalities decorated on graphene flakes. For the same kind of functionalized graphene membranes, the interlayer spacing and the general structure of the membranes are identical. Therefore, the different permeations of Cu^{2+} and Mg^{2+} through the same functionalized graphene membranes can be attributed to the different ion-functionality interactions. For each group of experiments, at least three runs are repeated. We find that excellent reproducibility can be achieved and that the variations of the

data are within the size of the data balls. Prior to the investigation on ion permeation through GO, G-OH, G-COOH, and G-NH₂ membranes with the cellulose microfilters underneath, control experiments with blank microfilters are conducted, as shown in Figure S3 of the Supporting Information. It reveals that no obvious differences between the transmembrane permeations of Cu^{2+} and Mg^{2+} through the polymeric microfilters can be observed, indicating that the microfilters have no selectivity toward different ions. Then, the permeations of Cu^{2+} and Mg^{2+} ions through the above four kinds of functionalized graphene membranes are plotted as a function of time, as shown in Figure 4. Notably, substantial deviations occur between the permeations of Cu^{2+} and Mg^{2+} ions through the same functionalized graphene membranes. In detail, for the case of ion-permeating GO membranes (Figure 4a), which is shown as a reference for the other three functionalized graphene membranes, the permeation of Mg^{2+} is greater than Cu^{2+} . This is in consistent with our previous work^{13,14} in which we proposed that the coordination between Cu^{2+} and the sp^3 C-O matrix of GO sheets should be stronger than the cation- π interaction between Mg^{2+} and the sp^2 nanocapillaries within GO membranes, further leading to the

effective capture of Cu^{2+} by GO membranes and the slower permeation of Cu^{2+} than Mg^{2+} . This inference can be further demonstrated experimentally by the permeation of Cu^{2+} and Mg^{2+} cations through G–OH and G–COOH membranes. As shown in Figure 4b and c, the permeation of Cu^{2+} is faster than Mg^{2+} when permeating through G–OH membranes, while the permeation of Mg^{2+} is significantly faster than Cu^{2+} when permeating through G–COOH membranes. We recall that the XPS spectrum of G–OH membranes in Figure 3b demonstrates the attachment of only a small portion of C–OH and C–O groups on the graphene flakes and the significant enhancement of the atomic ratio of sp^2 C–C regions. This indicates that the dominant cation– π interactions present between Mg^{2+} ions and the sp^2 clusters in G–OH membranes are responsible for the slower penetration of Mg^{2+} than Cu^{2+} ions, which is in agreement with our previous first-principles calculations.¹⁴

On the other hand, for G–COOH membranes, the XPS spectrum shows that the atomic percentage of carboxyl groups is significantly higher than GO membranes (Figure 3a and c). When it comes to ion permeating through GO and G–COOH membranes, the transmembrane permeation of Cu^{2+} ions is significantly weakened with the increase of the amount of carboxyl groups, further demonstrating that the strong coordination interactions between Cu^{2+} ions and carboxyl groups are indeed responsible for the weakened permeation of transition metallic Cu^{2+} ions through GO and G–COOH membranes. Notably, when grafting amino groups on GO basal planes, the deviations between the permeations of Cu^{2+} and Mg^{2+} cations are reduced obviously, as shown in Figure 4d. This indicates that the different chemical interactions of Cu^{2+} and Mg^{2+} cations with functionalized graphene no longer dominate the ion selectivity of G– NH_2 membranes. Instead, we propose that the significant electrostatic repulsions between metallic cations and the positive charges that originated from the strong attraction of H^+ by the N atoms in the amino groups begin to take effect. This can also be inferred from the slower permeation rates of Cu^{2+} and Mg^{2+} cations through G– NH_2 membranes than through GO membranes, as shown in Figure 4a and d. Moreover, the differences between ion permeations through G– NH_2 and GO membranes indicates that the modulation of ion transmembrane transportations can be achieved by grafting target functional groups on the graphene basal planes for diverse interactions between ions and graphene-based membranes.

Finally, the ion permeation rates of CuCl_2 and MgCl_2 sources through blank microfilters, GO, G–OH, G–COOH, and G– NH_2 membranes are extracted and shown in Figure 4e and f, respectively. Surprisingly, the permeation rate of Cu^{2+} ions through G–OH membrane with the cellulose microfilter underneath is even higher than through blank microfilter (Figure 4e). A similar phenomenon also occurs in the case of Mg^{2+} ions permeating through G–COOH/microfilter and blank microfilter, as shown in Figure 4f. The anomalous acceleration of ion transmembrane permeations might originate from the existence of rather weak binding interactions (between Cu^{2+} and sp^2 clusters in G–OH membranes and between Mg^{2+} ions and carboxyl groups in G–COOH membranes) but strong electrostatic attractions of cations with ionized oxygen-containing functional groups and electron-enriched π clusters, which result in the enrichment of cations around the negatively charged graphene-based membranes and

which further the fast transport of cations through the membranes.

In summary, the ion transmembrane permeations through GO, G–OH, G–COOH, and G– NH_2 membranes are investigated from which the delicate chemical interactions between different small ions and functionalized graphene are demonstrated to be responsible for the selectivity of graphene-based membranes, beyond the functioning range of molecular sieving effect (hydrated radii < 4.5 Å).⁷ In detail, the coordination interactions of transition-metal cations with carboxyl groups and the cation– π interactions of main-group cations with the sp^2 clusters take effect in recognizing different ions in solutions by graphene-based membranes. Notably, when grafting amino groups on GO basal planes, the ion permeations are weakened, indicating that the modulation of ion transportations through graphene-based membranes can be achieved by attaching with target functional groups. The results presented here not only throw light upon the mechanism for the selective ion permeation through graphene-based membranes but also lay a foundation for the separation of target ions by grafting specific functionalities.

■ ASSOCIATED CONTENT

§ Supporting Information

Permeation experiment detail, SEM images of GO materials and the permeation result through blank microfilters. This material is available free of charge via the Internet at <http://pubs.acs.org>.

■ AUTHOR INFORMATION

Corresponding Author

*E-mail: hongweizhu@tsinghua.edu.cn.

Notes

The authors declare no competing financial interest.

■ ACKNOWLEDGMENTS

This work is supported by Beijing Natural Science Foundation (2122027), National Program on Key Basic Research Project (2011CB013000), National Science Foundation of China (51372133), Tsinghua University Initiative Scientific Research Program (2012Z02102).

■ REFERENCES

- (1) Koenig, S. P.; Wang, L.; Pellegrino, J.; Bunch, J. S. Selective Molecular Sieving through Porous Graphene. *Nat. Nanotechnol.* **2012**, *7*, 728–732.
- (2) Garaj, S.; Liu, S.; Golovchenko, J. A.; Branton, D. Molecule-Hugging Graphene Nanopores. *Proc. Natl. Acad. Sci. U.S.A.* **2013**, *110*, 12192.
- (3) Cohen-Tanugi, D.; Grossman, J. C. Water Desalination across Nanoporous Graphene. *Nano Lett.* **2012**, *12*, 3602–3608.
- (4) Kim, H. W.; Yoon, H. W.; Yoon, S. M.; Yoo, B. M.; Ahn, B. K.; Cho, Y. H.; Shin, H. J.; Yang, H.; Paik, U.; Kwon, S.; et al. Selective Gas Transport Through Few-Layered Graphene and Graphene Oxide Membranes. *Science* **2013**, *342*, 91–95.
- (5) Li, H.; Song, Z.; Zhang, X.; Huang, Y.; Li, S.; Mao, Y.; Ploehn, H. J.; Bao, Y.; Yu, M. Ultrathin, Molecular-Sieving Graphene Oxide Membranes for Selective Hydrogen Separation. *Science* **2013**, *342*, 95–98.
- (6) Nair, R. R.; Wu, H. A.; Jayaram, P. N.; Grigorieva, I. V.; Geim, A. K. Unimpeded Permeation of Water Through Helium-Leak-Tight Graphene-Based Membranes. *Science* **2012**, *335*, 442–444.
- (7) Joshi, R. K.; Carbone, P.; Wang, F. C.; Kravets, V. G.; Su, Y.; Grigorieva, I. V.; Wu, H. A.; Geim, A. K.; Nair, R. R. Precise and

Ultrafast Molecular Sieving through Graphene Oxide Membranes. *Science* **2014**, 343, 752–754.

(8) Dikin, D. A.; Stankovich, S.; Zimney, E. J.; Piner, R. D.; Dommett, G. H. B.; Evmenenko, G.; Nguyen, S. T.; Ruoff, R. S. Preparation and Characterization of Graphene Oxide Paper. *Nature* **2007**, 448, 457–460.

(9) Eda, G.; Fanchini, G.; Chhowalla, M. Large-Area Ultrathin Films of Reduced Graphene Oxide as a Transparent and Flexible Electronic Material. *Nat. Nanotechnol.* **2008**, 3, 270–274.

(10) Eda, G.; Chhowalla, M. Chemically Derived Graphene Oxide: Towards Large-Area Thin-Film Electronics and Optoelectronics. *Adv. Mater.* **2010**, 22, 2392–2415.

(11) Loh, K. P.; Bao, Q.; Eda, G.; Chhowalla, M. Graphene Oxide as a Chemically Tunable Platform for Optical Applications. *Nat. Chem.* **2010**, 2, 1015–1024.

(12) Boukhvalov, D. W.; Katsnelson, M. I.; Son, Y. W. Origin of Anomalous Water Permeation through Graphene Oxide Membrane. *Nano Lett.* **2013**, 13, 3930–3935.

(13) Sun, P.; Zhu, M.; Wang, K.; Zhong, M.; Wei, J.; Wu, D.; Xu, Z.; Zhu, H. Selective Ion Penetration of Graphene Oxide Membranes. *ACS Nano* **2013**, 7, 428–437.

(14) Sun, P.; Zheng, F.; Zhu, M.; Song, Z.; Wang, K.; Zhong, M.; Wu, D.; Little, R. B.; Xu, Z.; Zhu, H. Selective Trans-Membrane Transport of Alkali and Alkaline Earth Cations through Graphene Oxide Membranes Based on Cation- π Interactions. *ACS Nano* **2014**, 8, 850–859.

(15) Sun, P.; Wang, K.; Wei, J.; Zhong, M.; Wu, D.; Zhu, H. Effective Recovery of Acids from Iron-Based Electrolytes Using Graphene Oxide Membrane Filters. *J. Mater. Chem. A* **2014**, 2, 7734–7737.

(16) Hummers, W. S.; Offeman, R. E. Preparation of Graphitic Oxide. *J. Am. Chem. Soc.* **1958**, 80, 1339.

(17) Yan, L.; Lin, M.; Zeng, C.; Chen, Z.; Zhang, S.; Zhao, X.; Wu, A.; Wang, Y.; Dai, L.; Qu, J.; et al. Electroactive and Biocompatible Hydroxyl-Functionalized Graphene by Ball Milling. *J. Mater. Chem.* **2012**, 22, 8367–8371.

(18) Liu, Y.; Deng, R.; Wang, Z.; Liu, H. Carboxyl-Functionalized Graphene Oxide–Polyaniline Composite as a Promising Supercapacitor Material. *J. Mater. Chem.* **2012**, 22, 13619–13624.

(19) Zhang, C.; Hao, R.; Liao, H.; Hou, Y. Synthesis of Amino-Functionalized Graphene as Metal-Free Catalyst and Exploration of the Roles of Various Nitrogen States in Oxygen Reduction Reaction. *Nano Energy* **2013**, 2, 88–97.